Conformal Singularities and Topological Defects from Inverse Transformation Optics

Lin Xu,[1,2,3] Runqiu He,[2] Kan Yao,[4] Jing Ming Chen,[2] Chong Sheng,[2] Ying Chen,[1] Guoxiong Cai,[1] Shining Zhu,[2] Hui Liu,[2,*] and Huanyang Chen[1,†]

[1]*Institute of Electromagnetics and Acoustics and Key Laboratory of Electromagnetic Wave Science and Detection Technology, Xiamen University, Xiamen 361005, China*

[2]*National Laboratory of Solid State Microstructures and School of Physics, Collaborative Innovation Center of Advanced Microstructures, Nanjing University, Nanjing, Jiangsu 210093, China*

[3]*Institutes of Physical Science and Information Technology, Key Laboratory of Opto-Electronic Information Acquisition and Manipulation of Ministry of Education, Anhui University, Hefei 230601, China*

[4]*Department of Mechanical Engineering and Texas Materials Institute, the University of Texas at Austin, Austin, Texas 78712, USA*

(Received 21 September 2018; revised manuscript received 13 February 2019; published 29 March 2019)

The conventional approach in transformation optics (TO) starts with a virtual space and determines a complicated material profile in physical space to achieve unconventional phenomena, such as invisibility cloaks. We demonstrate that complicated materials can be effectively fabricated by virtual space based on the reversed process of TO in two dimensions. We first show that a conformal singularity of a refractive-index profile, with either zero or infinity resulting from a power conformal mapping $w = z^{\alpha}$, is equivalent to a topological defect with positive charge or negative charge. The splitting effect and illusion effect are induced by the conformal singularities and related to the two-dimensional topological defects. Based on the equivalence, we fabricate a device of such a topological defect with a positive charge in experiments. Moreover, we observe its related light-bending functionality with laser beams. It has potential important applications in designing on-chip optical devices.

DOI: 10.1103/PhysRevApplied.11.034072

I. INTRODUCTION

The functionality of conventional lenses, such as glasses, is determined by the geometric shape of a material with fixed isotropic and homogeneous index of refraction properties. In the past decade, transformation optics (TO) has turned this around, such that the functionality of a designed material is instead determined by its anisotropy and inhomogeneity [1–4]. The marriage between TO and metamaterial engineering has drawn much attention, and many devices such as invisibility cloaks [5,6], field rotators [7,8], concentrators [9,10], and gravitational lensing [11,12] have been implemented. The "transformation" method, an inverse problem for determining the structural components of a system, is quite generic and has subsequently been transferred to other physical fields, such as acoustic waves [13–15] and thermal diffusions [16–20].

Intrinsically, TO deals with the connection between virtual space and physical space [1]. For virtual space, the light propagation is usually simple and obvious, while for physical space, the light propagation is complicated and peculiar due to the special material parameters. Most studies are focusing on designing devices in physical space. However, there are dispersion and dissipation of materials, which limit the engineering of TO [5]. Moreover, there are material singularities in TO-based devices [2] and other optical devices [21], which hinder their fabrications in practice. It is worth mentioning that some material singularities can be transmuted to anisotropic material by TO [21–23], which makes experiments more feasible. Such a transmutation method has been further developed to include an alternative concept, which is related to sculpted surfaces with local refractive-index profiles [24]. In two-dimensional (2D) space, conformal transformation optics (CTO) is proposed to manipulate light rays, which only requires materials with inhomogeneous isotropic refractive-index profiles [1,25]. For example, a conformal waveguide was recently designed and realized in the visible region [26]. There are also singularities in refractive-index profiles of optical devices, such as a zero value in a conformal cloaking device [1,25] and an infinity value in an invisible sphere [27]. A waveguide platform was proposed to elaborately design singularities of inhomogeneous refractive-index profiles [28]. However, those

*liuhui@nju.edu.cn
†kenyon@xmu.edu.cn

2D singularities still challenge the fabrication of optical devices.

Can we further combine the simplicity of virtual space together with devices in physical space to ease this implementation, such as singularities of inhomogeneous refractive-index profiles? Before nailing down the answer, we would like to recall some recent work. For example, the equivalence between a radial anisotropic material and a topological defect in three-dimensional (3D) space was built by an anholonomic transformation based on TO [29]. This topological defect is a TO-based analogue of cosmic string [30,31], which has been widely investigated both theoretically [32,33] and experimentally based on rotational anisotropic metasurfaces [34].

Here, we will prove that such a topological defect in virtual space is equivalent to a conformal singularity in physical space based on CTO. By embedding such a singularity in a uniform background, we can obtain a continuous refractive-index distribution, which then becomes finite in size. The splitting effect and illusion effect are demonstrated on the functionalities of these conformal singularities. The usual approach in TO starts with a virtual space and determines a material in physical space. Here, we inversely show that a complicated device can be achieved by virtual space. We construct such a topological defect by combining a cone together with a flat sheet following an artificial Riemann sheet [35] and experimentally demonstrate its light-bending functionality.

II. CONFORMAL SINGULARITY AND 2D TOPOLOGICAL DEFECT

Let us start with a power mapping written as

$$w = z^{\alpha}, \tag{1}$$

where α is a parameter (positive number) representing the topological property of this mapping. When $0 < \alpha < 1$, physical space and virtual space denoted as z and w complex planes are shown with axial grids in Figs. 1(a) and 1(b), respectively. Since α is less than 1, there is a missing section bounded with branch cuts (in yellow) of the Riemann surface shown in Fig. 1(b).

In order to connect light rays in both spaces, we suppose that the refractive-index profile in virtual space is uniform, namely, $n(w) = 1$. According to CTO [1], the corresponding refractive-index profile in physical space is

$$n(z) = n(w)|dw/dz| = \alpha r^{\alpha-1}. \tag{2}$$

The values of $n(z)$ and $n(w)$ are shown with contour plots in Figs. 1(a) and 1(b). We can further construct a cone structure by gluing two branch cuts of virtual space, as shown in Fig. 1(c). Such a cone structure is a flat space with a topological defect at the conical point. The conical point is a singularity, which gives rise to the special geometrical property. The coordinate of any point in the cone is (s, ρ), where s denotes the length from the conical point along the generatrix and ρ represents the distance from the rotational axis of the cone. Here, we want to mention that the refractive-index profiles of symmetrical media correspond to that of an equivalent geodesic lens [34], where $ds = ndr$, $\rho = nr$ is applied [36,37]. Under Eq. (2), we obtain $\rho = \alpha s$. Therefore, the geodesic lens of $n(z)$ of Eq. (2) shown in Fig. 1(a) is exactly a conical structure in Fig. 1(c), which is locally flat except for the conical topological defect. This method to achieve a cone surface with a local refractive-index profile for waves has been reported in Ref. [24] (not the power mapping here).

In physical space as shown in Fig. 1(a), there is a singularity with infinity at the center and the refractive index

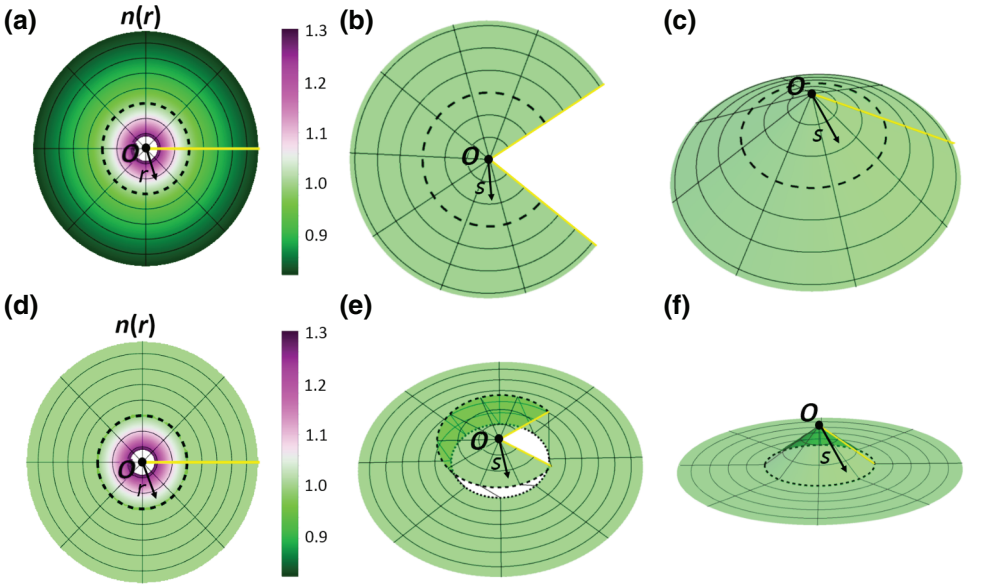

FIG. 1. Infinite conformal singularity and positive 2D topological defect. (a) Physical space and (b) virtual space of power conformal mapping $w = z^{\alpha}$ with $0 < \alpha < 1$. (c) Geodesic lens of physical space. (d) Physical space and (e) virtual space under truncation. (f) Geodesic lens of physical space under truncation.

with 1 is at the radius

$$r_0 = (1/\alpha)^{1/(\alpha-1)}, \tag{3}$$

which is described with the dashed black circle. Its images in Figs. 1(b) and 1(c) are dashed black arcs with a radius

$$r_1 = (1/\alpha)r_0. \tag{4}$$

The angle of the missing section is

$$\Delta\theta = 2\pi(1-\alpha), \tag{5}$$

which represents the topological defect of Eq. (1). Notice that the refractive index profile of Fig. 1(a) is filled in the whole space. We can simply choose a truncation with a radius r_0 such that the device becomes finite with a refractive-index profile from 1 to infinity inside r_0, and a unity refractive index outside r_0 as shown in Fig. 1(d). Owing to the truncation in physical space, the virtual space is also truncated at r_1, which should be connected to the region outside r_0 as shown in Fig. 1(d). Therefore, we obtain the new virtual space in Fig. 1(e), which can be regarded as an artificial Riemann sheet [35]. By gluing branch cuts in yellow, we get a rotational-symmetrical 2D surface in Fig. 1(f), which could be regarded as the geodesic lens of Fig. 1(d). It is worth mentioning that the truncation is not unique. One can arbitrarily choose a radius with the refractive index outside carefully designed to be globally continuous such that there is no reflection resulting from discontinuity of the refractive-index profile. Notice that various kinds of singular refractive-index profiles (such as Eaton lens and invisible lens, not from transformation optics) could be implemented by conelike surfaces with local refractive indices, showing that the geometry and refractive-index profile together can mimic another refractive-index profile. Here, we show that geometry itself can make this and is closely related to CTO in an inverse process.

Under the condition of $0 < \alpha < 1$, we successfully construct a rotational-symmetrical continuous inhomogeneous refractive-index profile with infinite singularity and a 2D surface with a positive topological defect. They both can be embedded in a uniform background.

When $\alpha > 1$, the values of $n(z)$ and $n(w)$ are shown with contour plots in Figs. 2(a) and 2(b), respectively. The singularity of the refractive-index profile in Fig. 2(a) is of zero value, which is different from that in Fig. 1(a). However, we can still conceive its virtual space as a Riemann surface as shown in Fig. 2(b), which has an additional section (in shadow) compared to a missing section in Fig. 1(b). The additional section is associated with a topological defect with a negative value according to Eq. (5), where $\alpha > 1$. A similar trick is also performed here. By setting the region outside r_0 to be 1, we can obtain a refractive-index profile in physical space from 0 to 1 as shown in Fig. 2(c) and

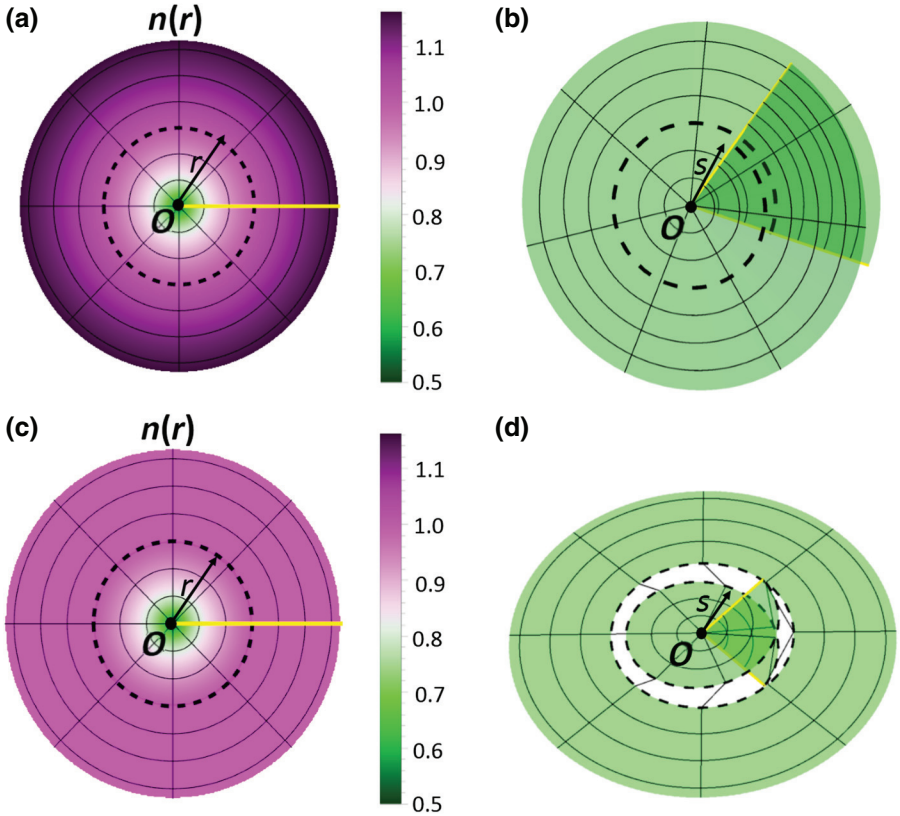

FIG. 2. Zero conformal singularity and negative 2D topological defect. (a) Physical space and (b) virtual space of power conformal mapping $w = z^{\alpha}$ with $\alpha > 1$. (c) Physical space and (d) virtual space under truncation.

a new virtual space in Fig. 2(d), or an artificial Riemann sheet. We cannot construct a similar structure in Figs. 1(c) and 1(f) in this case because of the additional section in virtual space. Nevertheless, we construct a rotational-symmetrical continuous inhomogeneous refractive-index profile with a singularity of zero and a 2D surface with a negative topological defect in a uniform background. Notice that there are similar methods of truncations for anisotropic profiles [38], which are different from the isotropic profiles here.

III. SPLITTING EFFECT AND ILLUSION EFFECT

Conformal singularities as well as their equivalent 2D topological defects can be used to control the propagation of light waves. Here, we demonstrate their splitting effect and illusion effect. We perform all the numerical simulations with commercial software COMSOL Multiphysics. A Gaussian beam is impinging on the singularity of infinity of Fig. 1(d). The splitting effect is observed as shown in Fig. 3(a), where the Gaussian beam seems attracted by the singularity of infinity to form two beams, which further go across each other and split away. Similarly, a Gaussian beam impinging on the singularity of zero of Fig. 2(c) is repelled to form two beams as shown in Fig. 3(d). The splitting effect is also confirmed by the trajectories in red and in blue as shown in Figs. 3(b) and 3(e), where parallel light rays impinge on those singularities with a tiny deviation. The splitting angle β is associated with α and $\Delta\theta$, which could be written as

$$\beta = \frac{\Delta\theta}{\alpha}. \tag{6}$$

We also plot the corresponding light rays in the geodesic surface of conformal singularities with a positive

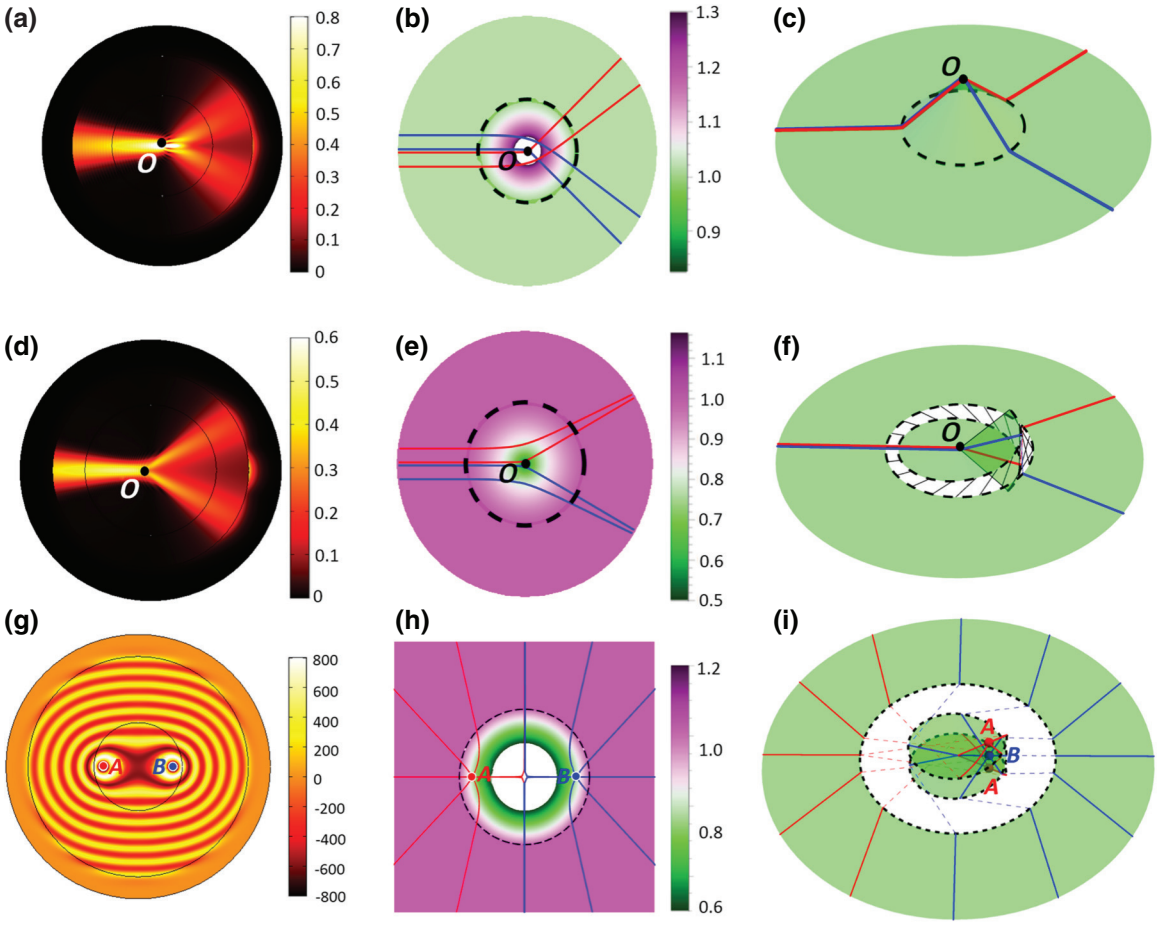

FIG. 3. Splitting effect and illusion effect. (a) The electric field pattern along the z direction of a Gaussian beam impinging on the infinite conformal singularity under truncation. (b) Light trajectories near the infinite conformal singularity under truncation. (c) Light trajectories near the geodesic lens of an infinite conformal singularity under truncation. (d) The electric field pattern of a Gaussian beam impinging on the zero conformal singularity under truncation. (e) Light trajectories near the zero conformal singularity under truncation. (f) Light trajectories in virtual space of zero conformal singularity under truncation. (g) The electric field pattern of two point sources placed at A $(-0.8, 0)$ and B $(0.8, 0)$ in the zero conformal singularity with $\alpha = 2$ under truncation. (h) Light trajectories in the zero conformal singularity under truncation. (i) Light trajectories in virtual space of a zero conformal singularity under truncation.

topological defect in Fig. 3(c) and the virtual space corresponding to a negative topological defect in Fig. 3(f).

It is noticed that steering electromagnetic beams or rays with conical curvature singularities in 3D space and their realization scheme based on anisotropic metamaterials have been systematically investigated in Refs. [29] and [32]. Recently, a related experimental work has demonstrated the ability of such anisotropic media in controlling electromagnetic beams, which mimics the effect of cosmic strings very well [34]. Such an anholonomic transformation is in 3D space and will result in an anisotropic profile. The mapping here is a conformal power mapping in 2D space, which satisfies Cauchy-Riemann conditions. We focus on singularities with isotropic refractive-index profiles and their 2D topological defect, which is simpler and different from the 3D case.

For $\alpha = 2, 3, 4 \ldots$, if we place α number of point sources near conformal singularities symmetrically, it can approximately present an almost identical field pattern of a single-point source, combining several point sources into one. Such an illusion effect can also be achieved by another much more complicated conformal mapping [39]. Let us take $\alpha = 2$, for example, in Fig. 3(g). Two point sources (denoted with "A" and "B") of electric polarization along the z direction are placed in the positions of $(0, -0.8)$ and $(0, 0.8)$, respectively. The wavefront far from the singularities gradually changes into an approximate circle, as if there is no interference between the two sources. This effect can be well understood in the limit of geometry optics as shown in Fig. 3(h). In the artificial Riemann sheet of virtual space of Fig. 3(i), there is an additional section of an entire identical circular region because of the negative topological defect with $\alpha = 2$. Such two circular regions are connected to the two half spaces outside under the truncation technique. Therefore, the two sources in blue and red seem to be independently propagating in their own circular regions and thereby in each half space. As for the physical space of Fig. 3(g) with conformal singularities, it inherits the fact from virtual space with conformal mapping, namely, the two symmetrical point sources each propagate on their own half space without interfering with each other. However, if the two point sources are not placed symmetrically, they will interfere with each other to eliminate the illusion effect. Such a refractive-index profile, ranging from 0 to 1, is possible to fabricate by metamaterials with H fractals [40].

We further make a Riemann sheet analysis for the illusion effect above. As shown in Fig. 4, we plot virtual space and physical space of power conformal mapping $w = z^{\alpha}$ with $\alpha = 2$. The Riemann sheet in virtual space contains two complex planes denoted by two different colors in Fig. 4(a). The upper-half complex plane in blue is connected with the lower-half complex plane by the solid yellow line, which can be mapped to the left-half plane in the physical space of Fig. 4(b). The other complex plane

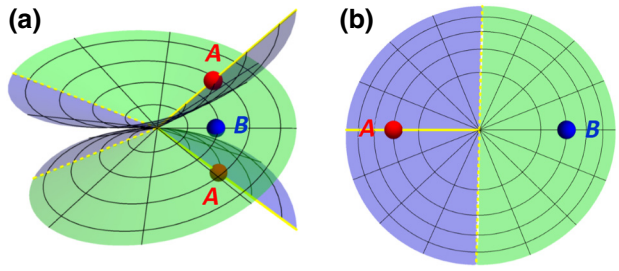

FIG. 4. (a) Physical space and (b) virtual space of power conformal mapping $w = z^{\alpha}$ with $\alpha = 2$.

(in green) of the Riemann sheet is mapped to the right-half plane in Fig. 4(b). The two complex planes are separated by the branch cut (denoted in dashed yellow lines). In virtual space, light rays from a point source B can only propagate in the complex plane in green and light rays from source A can only propagate in the complex plane in blue. Corresponding to the physical space in Fig. 4(b), light rays from A and B travel on their own half plane, which causes the illusion effect under the truncation as mentioned above.

IV. REALIZATION OF TOPOLOGICAL DEFECT

It is usually difficult to achieve conformal singularities of materials because of the wide range and extreme values of refractive-index profiles. Considering the equivalence between conformal singularities and 2D topological defects, we will construct a device with a 2D topological defect to manipulate light rays [Figs. 1(f) and 3(c)]. For example, we fabricate a waveguide sample with a conical surface structure. Our sample is a conical waveguide made of transparent resin. It is made of two parts, the conical part for bending light and the flat part for guiding light into the conical part. The shape and the size of the cone are clearly presented in Figs. 5(a) and 5(e), where the top view and side view of the sample are shown, respectively. The refractive index of the resin is around 1.56 when guiding visible light.

The scheme of optical measurement is shown in Fig. 6, where we use a laser beam with a wavelength of 405 nm. Between the laser and the sample, we use an aperture with an adjustable range from zero to 3000 μm to control the laser beam spot size. Then we adjust the six degrees-of-freedom platform to couple the beam into the sample and move it horizontally to guide the beam to impinge on the cone at different input positions. We use fluorescent imaging techniques to have a distinct view of the light paths inside the sample. In detail, two CCD cameras are placed in different locations. One is right above the sample while the other is perpendicular to the side surface to observe the side view. Both have a color filter to collect fluorescence.

The photos caught by the camera right above the sample based on fluorescent imaging techniques are shown in

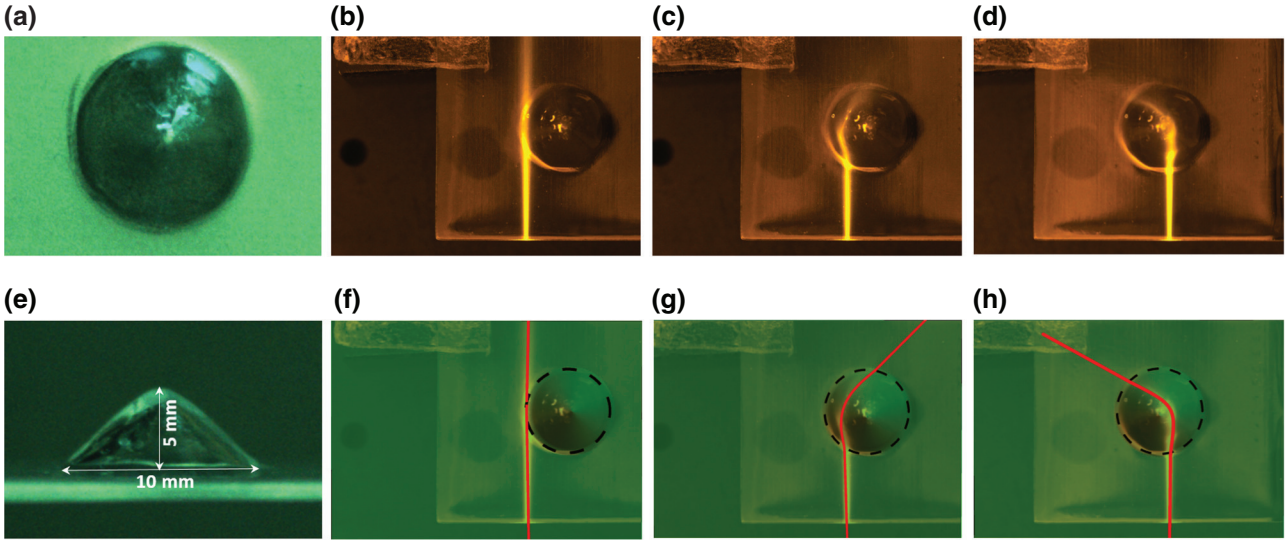

FIG. 5. The experimental pictures of the sample and the bending effect. (a) The top view of the sample. (e) The side view. The height and the diameter of the cone are 5 mm and 10 mm, respectively. (b–d) The laser beam impinges on the cone at different positions. They are bent by the 2D conical waveguide. (f–h) The corresponding fitting results with topological defects.

Fig. 5. The direction of the laser beam (in yellow) tangent to the cone boundary is not affected by the cone, which is shown in Fig. 5(b), while for other different impinging positions, the laser beam (in yellow) is gradually bent, as demonstrated by Figs. 5(c) and 5(d). We use the structure shown in Fig. 1(f) to fit the measurements of Figs. 5(b)–5(d) by the camera. The results in red curves are plotted in Figs. 5(f)–5(h), which match the experiments very well. Therefore, the topological defect of the conical structure can effectively perform as a conformal

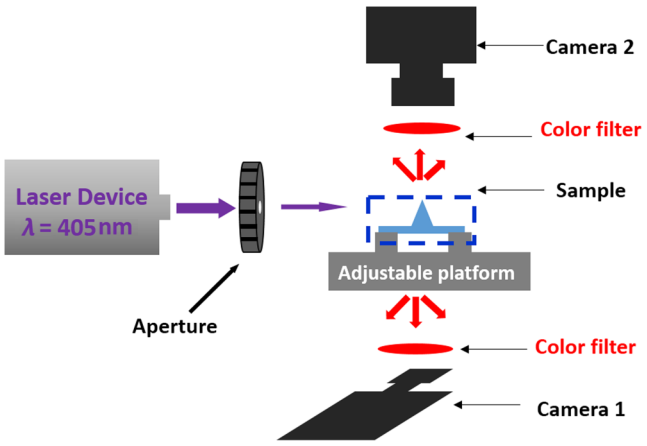

FIG. 6. Experimental set up schematic of the optical measurement. A laser beam is coupled to a 2D conical waveguide structure from the side face through an aperture. The fluorescent light is excited inside the waveguide by the laser beam to show the light path in the 2D CCD cameras. When the sample is moved horizontally relative to the beam, different light paths can be caught by the 2D CCD cameras.

singularity. There does, however, exist some loss induced by fluorescent imaging techniques, which can be removed in a real application without energy loss by conversion of the fluorescent source.

V. CONCLUSION

In summary, we find that the conformal singularities of a refractive-index profile, with either zero or infinity, which result from the conformal mapping $w = z^{\alpha}$, are equivalent to positive or negative topological defects. We truncate the devices of these singularities such that they can be embedded in a uniform background to form a continuous refractive-index distribution, which is also equivalent to a topological defect with a truncation in a uniform material. The splitting effect and illusion effect of these singularities and topological defects are confirmed by numerical simulations. We show that a conformal singularity can effectively be achieved by a 2D topological defect in virtual space. We fabricate such a device with a positive topological defect and demonstrate its functionality of light bending. Our work shows that a complicated device can be achieved in virtual space based on CTO. Since all curved surfaces are conformally flat [3], one can find a curved surface without rotational symmetry, which corresponds to a certain inhomogeneous refractive-index profile. This could be used as a platform to connect conventional geometric optics with on-chip applications [41]. For example, multiple conical structures could be arranged to guide light freely in 2D spaces. The design and fabrication of the cone surface can serve as a deflector for integrated photonics and microcavities for nonlinear optics based on the wave theory in Ref. [24] and current work on geometric optics.

In principle, our design may work on a broad band of frequencies, which has been a problem in previous metamaterials engineering. In addition, one can achieve similar results in a thin acoustic curved waveguide following our method.

ACKNOWLEDGMENTS

This work was financially supported by the National Natural Science Foundation of China (Grants No. 11874311, No. 11690033, No. 61425018, No. 11621091, and No. 11704181), National Key R&D Program of China (Grant No. 2017YFA0303702), National Key Research and Development Program of China (Grant No. 2017YFA0205700), and the Fundamental Research Funds for the Central Universities (Grant No. 20720170015).

L.X. and R.H. contributed equally to this work.

[1] U. Leonhardt, Optical conformal mapping, Science **312**, 1777 (2006).
[2] J. B. Pendry, D. Schurig, and D. R. Smith, Controlling electromagnetic fields, Science **312**, 1780 (2006).
[3] U. Leonhardt and T. Philbin, *Geometry and Light: The Science of Invisibility* (Dover Inc., Mineola, New York, 2010).
[4] H. Chen, C. T. Chan, and P. Sheng, Transformation optics and metamaterials, Nat. Mater. **9**, 387 (2010).
[5] D. Schurig, J. Mock, B. Justice, S. A. Cummer, J. B. Pendry, A. Starr, and D. Smith, Metamaterial electromagnetic cloak at microwave frequencies, Science **314**, 977 (2006).
[6] U. Leonhardt and T. Tyc, Broadband invisibility by non-Euclidean cloaking, Science **323**, 110 (2009).
[7] H. Chen and C. Chan, Transformation media that rotate electromagnetic fields, Appl. Phys. Lett. **90**, 241105 (2007).
[8] H. Chen, B. Hou, S. Chen, X. Ao, W. Wen, and C. Chan, Design and Experimental Realization of a Broadband Transformation Media Field Rotator at Microwave Frequencies, Phys. Rev. Lett. **102**, 183903 (2009).
[9] M. Rahm, D. Schurig, D. A. Roberts, S. A. Cummer, D. R. Smith, and J. B. Pendry, Design of electromagnetic cloaks and concentrators using form-invariant coordinate transformations of Maxwell's equations, Photonics Nanostruct. **6**, 87 (2008).
[10] M. M. Sadeghi, S. Li, L. Xu, B. Hou, and H. Chen, Transformation optics with Fabry-Pérot resonances, Sci. Rep. **5**, 8680 (2015).
[11] C. Sheng, H. Liu, Y. Wang, S. N. Zhu, and D. Genov, Trapping light by mimicking gravitational lensing, Nat. Photonics **7**, 902 (2013).
[12] C. Sheng, R. Bekenstein, H. Liu, S. N. Zhu, and M. Segev, Wavefront shaping through emulated curved space in waveguide settings, Nat. Commun. **7**, 10747 (2016).
[13] H. Chen and C. Chan, Acoustic cloaking in three dimensions using acoustic metamaterials, Appl. Phys. Lett. **91**, 183518 (2007).
[14] A. N. Norris, Acoustic cloaking theory, Proc. R. Soc. Lond. A **464**, 2411 (2008).
[15] H. Chen and C. T. Chan, Acoustic cloaking and transformation acoustics, J. Phys. D: Appl. Phys. **43**, 113001 (2010).
[16] C. Fan, Y. Gao, and J. Huang, Shaped graded materials with an apparent negative thermal conductivity, Appl. Phys. Lett. **92**, 251907 (2008).
[17] S. Narayana and Y. Sato, Heat Flux Manipulation with Engineered Thermal Materials, Phys. Rev. Lett. **108**, 214303 (2012).
[18] R. Schittny, M. Kadic, S. Guenneau, and M. Wegener, Experiments on Transformation Thermodynamics: Molding the Flow of Heat, Phys. Rev. Lett. **110**, 195901 (2013).
[19] T. Han, X. Bai, D. Gao, J. T. Thong, B. Li, and C.-W. Qiu, Experimental Demonstration of a Bilayer Thermal Cloak, Phys. Rev. Lett. **112**, 054302 (2014).
[20] H. Xu, X. Shi, F. Gao, H. Sun, and B. Zhang, Ultrathin Three-Dimensional Thermal Cloak, Phys. Rev. Lett. **112**, 054301 (2014).
[21] T. Tyc and U. Leonhardt, Transmutation of singularities in optical instruments, New J. Phys. **10**, 115038 (2008).
[22] I. R. Hooper and T. G. Philbin, Transmutation of singularities and zeros in graded index optical instruments: A methodology for designing practical devices, Opt. Express **21**, 32313 (2013).
[23] Y. Liu, M. Mukhtar, Y. Ma, and C. Ong, Transmutation of planar media singularities in a conformal cloak, J. Opt. Soc. Am. A **30**, 2280 (2013).
[24] S. Horsley, I. Hooper, R. Mitchell–Thomas, and O. Quevedo–Teruel, Removing singular refractive indices with sculpted surfaces, Sci. Rep. **4**, 4876 (2014).
[25] L. Xu and H. Chen, Conformal transformation optics, Nat. Photonics **9**, 15 (2014).
[26] X. Wang, H. Chen, H. Liu, L. Xu, C. Sheng, and S. Zhu, Self-Focusing and the Talbot Effect in Conformal Transformation Optics, Phys. Rev. Lett. **119**, 033902 (2017).
[27] J. C. Miñano, Perfect imaging in a homogeneous three-dimensional region, Opt. Express **14**, 9627 (2006).
[28] S. Viaene, V. Ginis, J. Danckaert, and P. Tassin, Mitigating optical singularities in coordinate-based metamaterial waveguides, Phys. Rev. B **95**, 155412 (2017).
[29] Y.-L. Zhang, X.-Z. Dong, M.-L. Zheng, Z.-S. Zhao, and X.-M. Duan, Steering electromagnetic beams with conical curvature singularities, Opt. Lett. **40**, 4783 (2015).
[30] T. W. Kibble, Topology of cosmic domains and strings, J. Phys. A: Math. Gen. **9**, 1387 (1976).
[31] N. D. Mermin, The topological theory of defects in ordered media, Rev. Mod. Phys. **51**, 591 (1979).
[32] Y.-L. Zhang, J. B. Pendry, and D. Y. Lei, Radial anisotropy from a geometric viewpoint: Topological singularity and effective medium realization, Phys. Rev. B **96**, 035430 (2017).
[33] I. Fernández-Núñez and O. Bulashenko, Wave propagation in metamaterials mimicking the topology of a cosmic string, J. Opt. **20**, 045603 (2018).
[34] C. Sheng, H. Liu, H. Chen, and S. Zhu, Definite photon deflections of topological defects in metasurfaces and symmetry-breaking phase transitions with material loss, Nat. Commun. **9**, 4271 (2018).
[35] L. Xu and H. Chen, Transformation optics with artificial Riemann sheets, New J. Phys. **15**, 113013 (2013).

[36] M. Šarbort and T. Tyc, Spherical media and geodesic lenses in geometrical optics, J. Opt. **14**, 075705 (2012).
[37] L. Xu, T. Tyc, H. Chen, Geodesic conformal transformation optics: manipulating light with continuous refractive index profile, arXiv preprint:1802.00913 (2018).
[38] M. Rahm, S. A. Cummer, D. Schurig, J. B. Pendry, and D. R. Smith, Optical Design of Reflectionless Complex Media by Finite Embedded Coordinate Transformations, Phys. Rev. Lett. **100**, 063903 (2008).
[39] H. Chen, Y. Xu, H. Li, and T. Tyc, Playing the tricks of numbers of light sources, New J. Phys. **15**, 093034 (2013).
[40] Q. Wu, X. Feng, R. Chen, C. Gu, S. Li, H. Li, Y. Xu, Y. Lai, B. Hou, H. Y. Chen, and Y. Li, An inside-out Eaton lens made of H-fractal metamaterials, Appl. Phys. Lett. **101**, 031903 (2012).
[41] T. Zentgraf, Y. Liu, M. H. Mikkelsen, J. Valentine, and X. Zhang, Plasmonic luneburg and eaton lenses, Nat. Nanotechnol. **6**, 151 (2011).